

## **Influence of Electrode Radius on Apparent Lability of Complex of Amalgam Forming Ions**

*Milivoj Lovrić\* and Šebojka Komorsky-Lovrić*

Department of Marine and Environmental Research, “Rudjer Bošković” Institute, 10000 Zagreb, Hrvatska (Croatia)

\*E-mail: [mlovric@irb.hr](mailto:mlovric@irb.hr)

*Received: 22 May 2014 / Accepted: 18 June 2014 / Published: 16 July 2014*

---

A theory of reversible electrode reaction preceded by the reversible chemical reaction is developed for square-wave voltammetry of amalgam forming ions on spherical electrode. It is shown that the lability parameter is diminished as the radius of electrode is decreased. This is in agreement with the previous calculations and shows that the diffusion of amalgam within the spherical electrode has no influence on the apparent lability of metal complex.

---

**Keywords:** Amalgam, metal ions, complex, spherical electrode, voltammetry

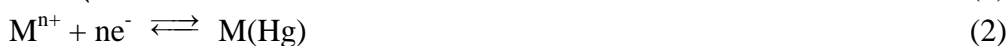
### **1. INTRODUCTION**

The interaction of trace metals with living organisms and suspended particles in natural waters depends on the distribution of their ionic species [1, 2]. In these media the metals are associated with inorganic and organic ligands, forming complexes of various strengths [3, 4]. Their bioavailability is determined by the concentrations of free ions and labile complexes [5]. The later species are characterized by such high rates of dissociation and association that full equilibrium between complexed and free ions is maintained under all conditions [6]. Analytical techniques applied to the speciation provide information about operationally defined fraction of trace metals with respect to the particular measurement procedure [7]. For the distinction between labile and inert complexes, voltammetric stripping techniques are widely employed [8, 9]. In these methods the lability is defined as the ratio between the fluxes of dissociation and diffusion of the complex [10]. It was shown theoretically that the apparent lability at spherical microelectrodes decreases as the electrode radius is decreasing [10, 11]. This is caused by the enhanced diffusion, while the kinetic flux is unaltered. This is confirmed by the analysis of CE mechanism on spherical electrodes [12 - 14]. The investigation of

this phenomenon is extended to electrode reactions of amalgam forming ions and the results are reported in this communication. In these reactions the diffusion of amalgam within the mercury drop must be taken in consideration [15 - 17]. Theoretical dependence of peak current and potential on the frequency and electrode radius is investigated in square-wave voltammetry. The chosen technique utilizes a combination of a staircase potential modulation and periodic square-shaped potential function [18]. It unifies the enhanced sensitivity of pulse techniques, the insight into the electrode mechanism of cyclic voltammetry and the information on kinetics of fast charge transfers [19, 20].

## 2. THE MODEL

It is assumed that in the bulk of solution there are an amalgam forming metal ion  $M^{n+}$ , a ligand  $L^{n-}$  and their complex ML and that the ion and the complex are connected by the first order dissociation and the second order complex formation kinetics. Finally, a reversible electrode reaction of free metal ions on mercury drop electrode is considered:



$$t = 0; r \geq r_m : c_{ML} = c_{ML}^*, c_M = c_M^*, c_L = c_L^*, c_{M(Hg)} = 0 \tag{3}$$

$$K_{eq} = c_{ML}^* (c_M^* c_L^*)^{-1} \tag{4}$$

$$0 \leq r < r_m : c_{ML} = 0, c_M = 0, c_L = 0, c_{M(Hg)} = 0 \tag{5}$$

$$t > 0; r \rightarrow \infty : c_{ML} \rightarrow c_{ML}^*, c_M \rightarrow c_M^*, c_L \rightarrow c_L^* \tag{6}$$

$$r = r_m : (c_M)_{r=r_m} = (c_{M(Hg)})_{r=r_m} \exp(\varphi) \tag{7}$$

$$\varphi = \frac{nF}{RT} (E - E^0) \tag{8}$$

$$D \left( \frac{\partial c_M}{\partial r} \right)_{r=r_m} = - \frac{I}{nFS} \tag{9}$$

$$D \left( \frac{\partial c_{M(Hg)}}{\partial r} \right)_{r=r_m} = - \frac{I}{nFS} \tag{10}$$

$$D \left( \frac{\partial c_{ML}}{\partial r} \right)_{r=r_m} = 0 \tag{11}$$

$$D \left( \frac{\partial c_L}{\partial r} \right)_{r=r_m} = 0 \tag{12}$$

$$r = 0 : \left( \frac{\partial c_{M(Hg)}}{\partial r} \right)_{r=0} = 0 \tag{13}$$

The meanings of symbols are the following:  $c_{ML}, c_M, c_L$  and  $c_{M(Hg)}$  are concentrations of the complex ML and ions  $M^{n+}$  and  $L^{n-}$  in the electrolyte and atoms M in the mercury, respectively,  $c_{ML}^*, c_M^*$  and  $c_L^*$  are the bulk concentrations of the complex and the ions,  $K_{eq}$  is the stability constant of the complex,  $E$  is electrode potential,  $E^0$  is standard potential of electrode reaction (2),  $D$  is a common diffusion coefficient,  $I$  is a current,  $n$  is a number of electrons,  $F$  is Faraday constant,  $S$  is the electrode surface area and  $r_m$  is the radius of mercury electrode.

The mass transport is calculated by the Feldberg approximation [21]:

$$\left( \frac{\Delta c_M}{\Delta t} \right)_i = D \left[ \frac{A_i}{V_i} \left( \frac{\Delta c_M}{\Delta r} \right)_{i+1,i} - \frac{A_{i-1}}{V_i} \left( \frac{\Delta c_M}{\Delta r} \right)_{i,i-1} \right] + k_f (c_{ML})_i - k_b (c_M)_i (c_L)_i \tag{14}$$

$$\left( \frac{\Delta c_{ML}}{\Delta t} \right)_i = D \left[ \frac{A_i}{V_i} \left( \frac{\Delta c_{ML}}{\Delta r} \right)_{i+1,i} - \frac{A_{i-1}}{V_i} \left( \frac{\Delta c_{ML}}{\Delta r} \right)_{i,i-1} \right] - k_f (c_{ML})_i + k_b (c_M)_i (c_L)_i \tag{15}$$

$$\left(\frac{\Delta c_L}{\Delta t}\right)_i = D \left[ \frac{A_i}{V_i} \left(\frac{\Delta c_L}{\Delta r}\right)_{i+1,i} - \frac{A_{i-1}}{V_i} \left(\frac{\Delta c_L}{\Delta r}\right)_{i,i-1} \right] + k_f(c_{ML})_i - k_b(c_M)_i(c_L)_i \quad (16)$$

$$\left(\frac{\Delta c_{M(Hg)}}{\Delta t}\right)_i = D \left[ \frac{A_i}{V_i} \left(\frac{\Delta c_{M(Hg)}}{\Delta r}\right)_{i+1,i} - \frac{A_{i-1}}{V_i} \left(\frac{\Delta c_{M(Hg)}}{\Delta r}\right)_{i,i-1} \right] \quad (17)$$

Here:  $A_i = 4\pi r_i^2$ ,  $A_{i-1} = 4\pi r_{i-1}^2$ ,  $V_i = \frac{4}{3}\pi(r_i^3 - r_{i-1}^3)$ ,  $r_i = i\Delta r$ ,  $r_m = m\Delta r$ ,  $k_f$  is the rate constant of dissociation of the complex and  $k_b = k_f K_{eq}$ . The simulation procedure is described in the Appendix. The results are reported as dimensionless current  $\Phi = I(nFS c_{tot}^*)^{-1}(Df)^{-1/2}$ . In square wave voltammetry the current is sampled at the end of each pulse and the difference between two subsequent samples is called the net response:  $\Delta\Phi = \Phi_f - \Phi_b$ . The forward, reductive ( $\Phi_f$ ) and the backward, oxidative ( $\Phi_b$ ) components of the net response are also reported as a function of the potential of staircase ramp.

The responses depend on the pulse amplitude  $E_{sw}$ , the potential step  $dE$ , the kinetics of chemical reaction and the inverse value of dimensionless electrode radius  $\rho = r_m^{-1}(D/f)^{1/2}$ . In the simulation each pulse is divided into 25 time increments and the dimensionless diffusion coefficient  $d = 0.4$  was used (see eq. A11). So, the parameter  $\rho$  depends on the number of space increments into which the electrode radius is divided:  $\rho = \sqrt{20}/m$ .

### 3. RESULTS AND DISCUSSION

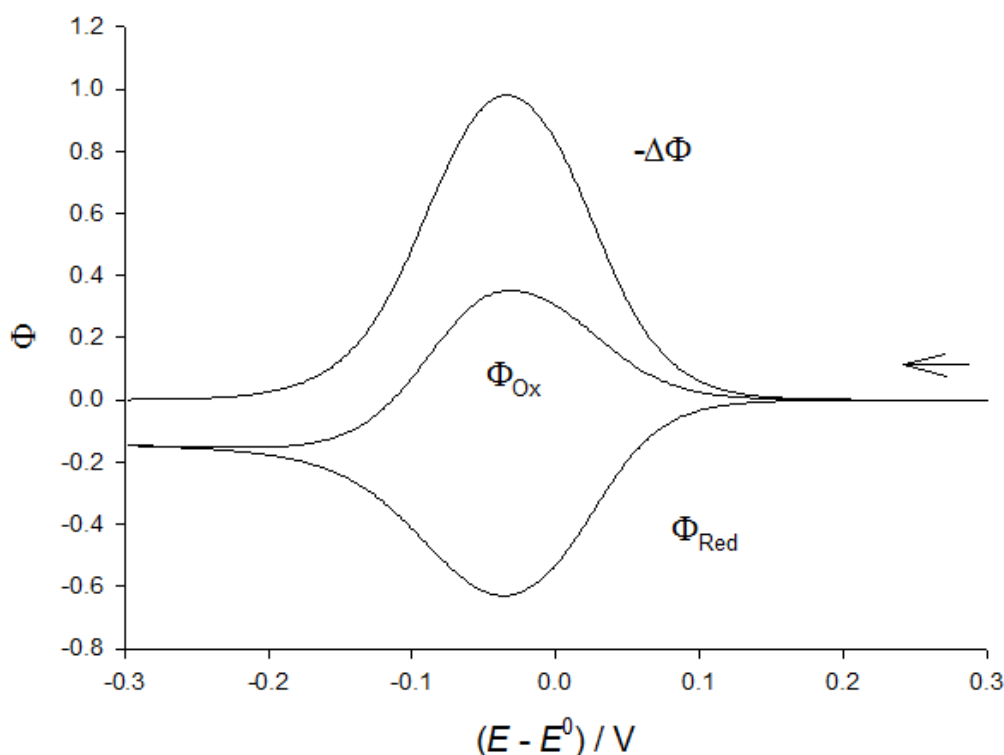


**Figure 1.** A theoretical dimensionless square wave voltammogram of electrode reaction (2). A negative net response ( $-\Delta\Phi$ ) and its forward ( $\Phi_{Red}$ ) and backward ( $\Phi_{Ox}$ ) components are shown.  $E_{st} = 0.3$  V vs.  $E^0$ ,  $E_{sw} = 50$  mV,  $dE = -2$  mV,  $\rho = 0.1$ ,  $k_f/f = 5$ ,  $K_{eq} = 10^3$  L/mol,  $c_L^* = 10^{-3}$  mol/L and  $c_{tot}^* = 10^{-4}$  mol/L.

Figure 1 shows an example of square wave voltammogram of electrode reaction (2). The dimensionless net peak current is 0.98 and the peak potential is  $-0.034 \text{ V vs. } E^0$ . The minimum and maximum of the reductive and oxidative components of the response appear at  $-0.036 \text{ V}$  and  $-0.030 \text{ V}$ , respectively. The limiting currents of both components tend to  $-\rho$  if  $E \ll E^0$ . However, the extremes of components do not vanish with the diminishing of electrode radius, as they do in the case of solution soluble product [22], because of the diffusion of amalgam that is restricted to the finite space within the drop [23].

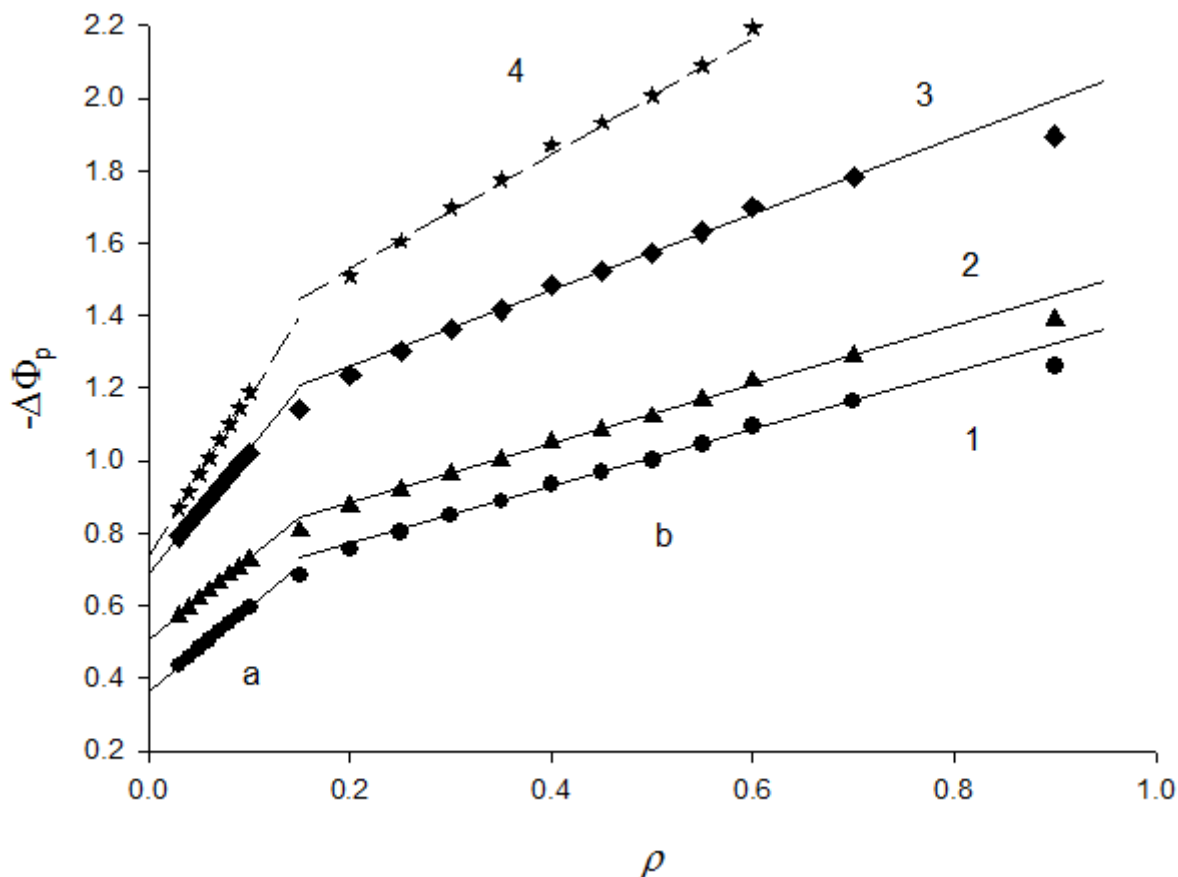


**Figure 2.** Dependence of dimensionless net peak current on the dimensionless inverse electrode radius;  $k_f/f = 0$  (1), 0.5 (2), 7.5 (3) and  $\rightarrow \infty$  (4). All other parameters are as in Fig. 1.

The relationships between net peak currents and the parameter  $\rho$  are shown in Fig. 2. They are curves with two asymptotes that are marked as (a) and (b). The curves (1) and (4) correspond to totally inert complex and to ideally labile complex, respectively. These two curves show dependence of pure diffusion flux density on electrode radius. In the case of inert complex, the current depends solely on the diffusion of free metal ions. Their bulk concentration is related to the total metal concentration by the following equation:  $c_M^* = c_{tot}^* (1 + K_{eq} c_L^*)^{-1}$ . For the product  $K_{eq} c_L^* = 1$ , the ratio  $c_M^*/c_{tot}^*$  is equal to 0.5. For this reason the slopes and intercepts of straight lines (a) and (b) in curve (4) are twice as big as the corresponding slopes and intercepts in curve (1). These values are as follows:  $-\Delta\Phi_p = 4.4 \rho + 0.74$  (4a),  $-\Delta\Phi_p = 2.2 \rho + 0.37$  (1a),  $-\Delta\Phi_p = 1.6 \rho + 1.2$  (4b) and

$-\Delta\Phi_p = 0.8\rho + 0.6$  (1b). They are in agreement with the results of calculations of simple electrode reaction [23]. Under the influence of dissociation of complex, the peak currents increase but their dependence on  $\rho$  does not change essentially. The asymptotes (a) and (b) in the curves (2) and (3) are given by the following equations:  $-\Delta\Phi_p = 2.15\rho + 0.50$  (2a),  $-\Delta\Phi_p = 3.4\rho + 0.7$  (3a),  $-\Delta\Phi_p = 0.8\rho + 0.7$  (2b) and  $-\Delta\Phi_p = 1.05\rho + 1.05$  (3b). Considering the definitions of  $\rho$  and the surface area of hemispherical microelectrodes, these straight lines indicate the dependence of the real net peak current on electrode radius and frequency. For instance, the line (3b) can be transformed into the following equation:

$$-\Delta I_p = 2\pi n F c_{tot}^* r_m \sqrt{D} (1.05 r_m \sqrt{f} + 1.05 \sqrt{D}) \tag{18}$$

However, the number 1.05 in the brackets of eq. (18) is the function of the ratio  $k_f/f$ , which is the dimensionless rate constant of dissociation of complex. This shows that the relationship between  $-\Delta I_p$  and the square-root of frequency is a curve that does not pass through the origin.

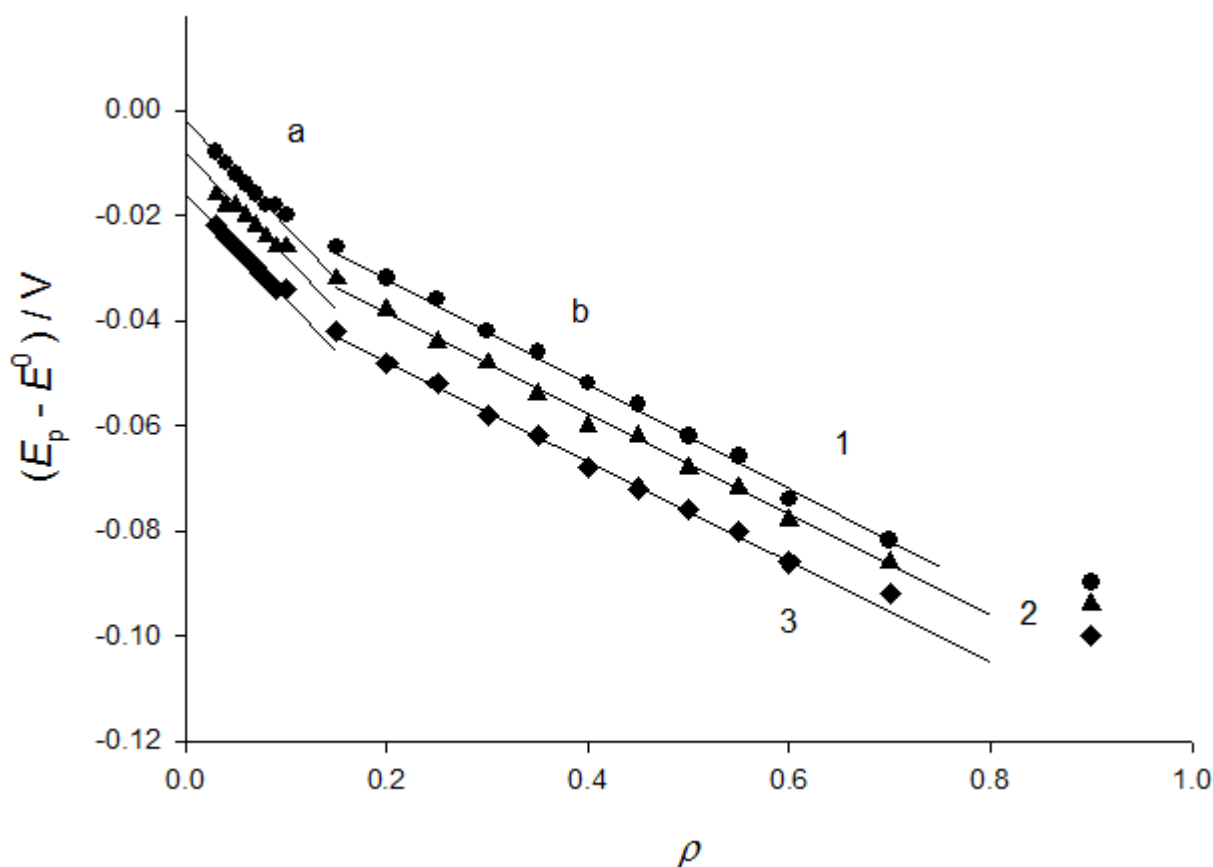


**Figure 3.** Dependence of net peak potentials on the dimensionless inverse electrode radius;  $k_f/f = 0$  (1), 0.5 (2) and 7.5 (3). All other parameters are as in Fig. 1.

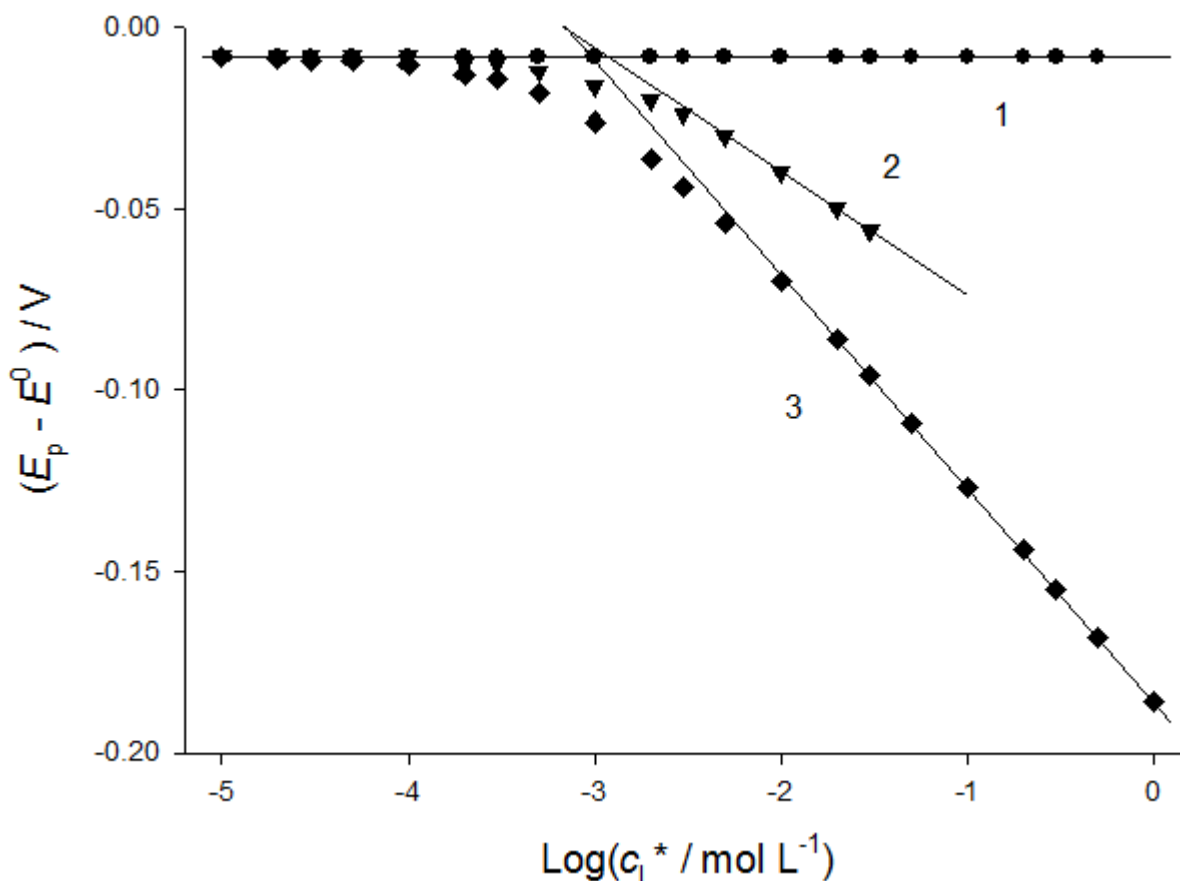
Fig. 3 displays the dependence of peak potential of the net response on the parameter  $\rho$ . The straight lines (a) and (b) in this figure are defined by the following equations:  $E_p - E^0 = -0.2\rho - z$  (V) and  $E_p - E^0 = -0.1\rho - z$  (V). The values of the intercept  $z$  increase proportionally to the dimensionless rate constant of dissociation: 0.002 (1a), 0.008 (2a), 0.016 (3a),

0.012 (1b), 0.019 (2b) and 0.029 (3b). These shifts of peak potentials are caused by the energy that is needed for the partial dissociation of the complex. This phenomenon can be used for the determination of stability constant of the complex by the method of DeFord and Hume [24]. The relationship between peak potentials and the logarithm of concentration of ligand is shown in Fig. 4 for three types of complexes and two values of sphericity parameter. If the complex is totally inert, the peak potential is independent of the ligand concentration. The dependence of  $E_p$  on  $\log c_L^*$  of ideally labile complex is a curve that tends to the asymptote:

$$E_p = (E_p)_{c_L^* \rightarrow 0} - 0.059 \log K_{eq} - 0.059 \log c_L^* \tag{19}$$

The cross section of this asymptote and the straight line  $E_p = (E_p)_{c_L^* \rightarrow 0}$  determines the logarithm of stability constant:  $\log K_{eq} = -(\log c_L^*)_{\text{cross}}$ . This cross section is independent of the parameter  $\rho$ . In the general case the peak potential is a function of the kinetics of dissociation of complex as well as of the ligand concentration and dimensionless electrode radius. This is shown by the curve (2) in Fig. 4. If  $\rho = 0.03$  this curve tends to the straight line:

$$E_p = (E_p)_{c_L^* \rightarrow 0} - 0.034 \log K_{eq} - 0.034 \log c_L^* \tag{20}$$



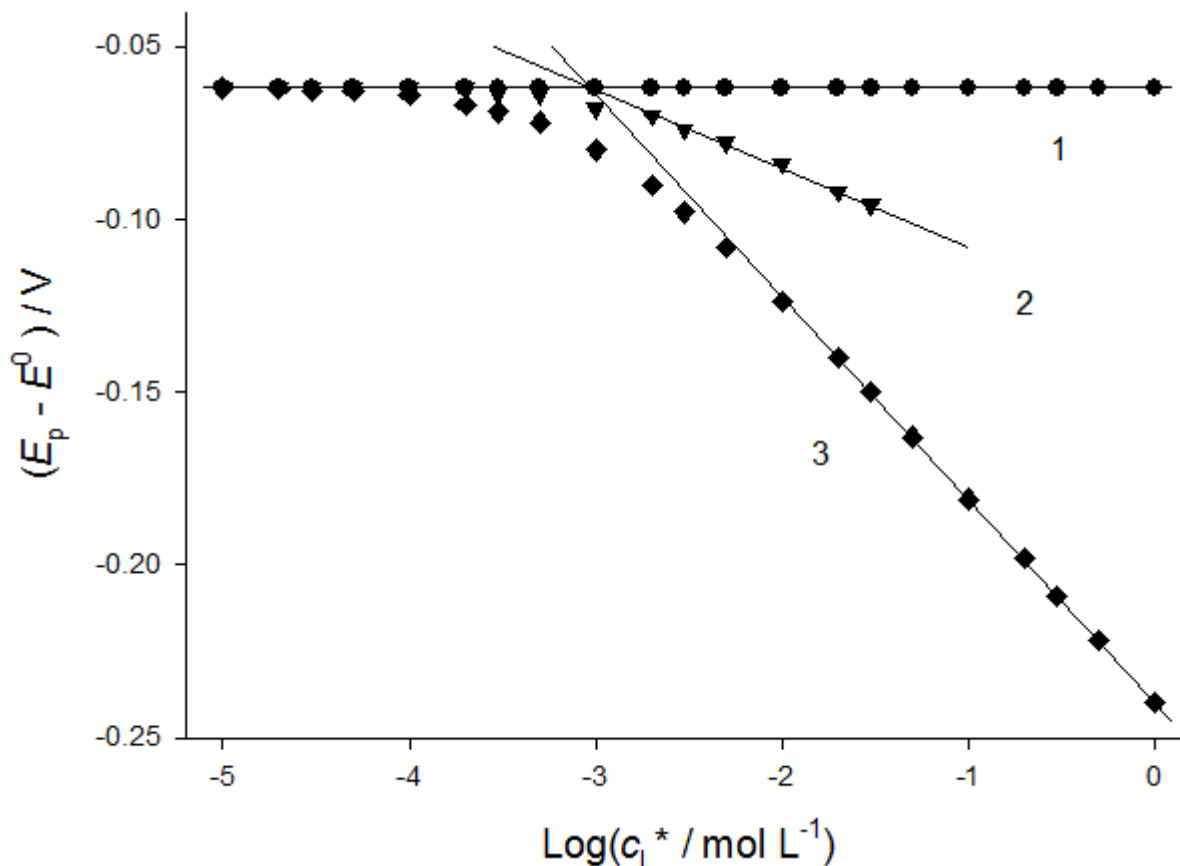


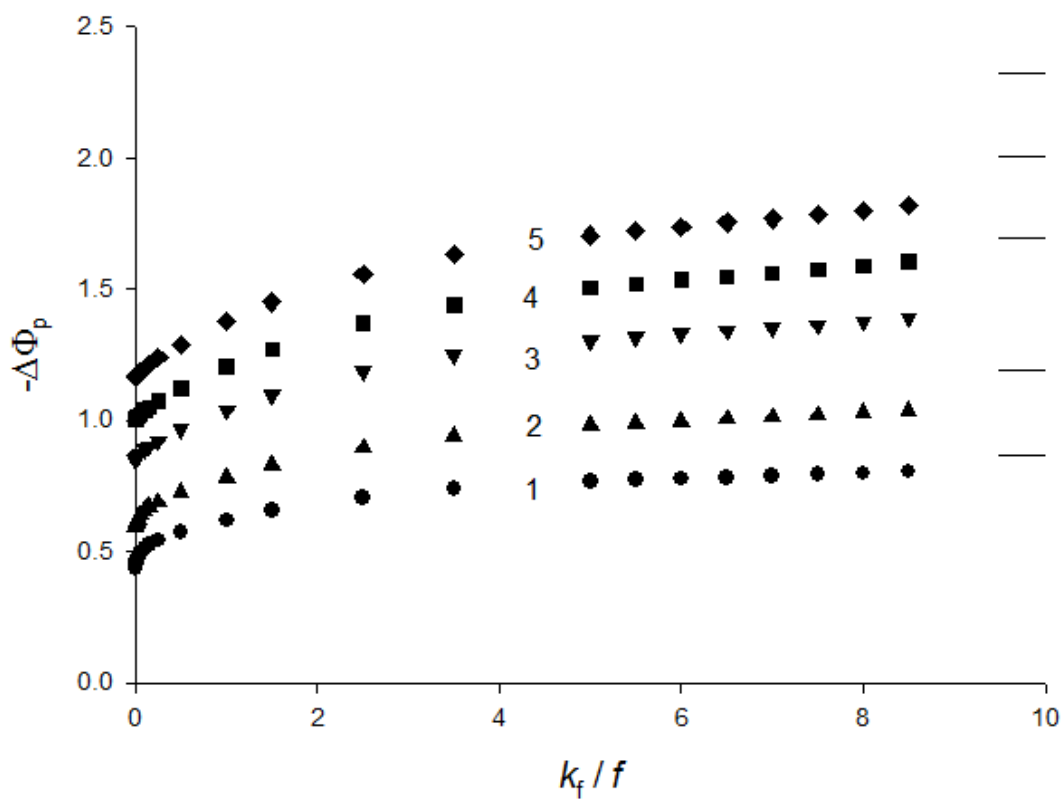
**Figure 4.** Dependence of peak potential on the logarithm of ligand concentration;  $\rho = 0.03$  (A) and 0.5 (B);  $k_f/f = 0$  (1), 0.5 (2) and  $\rightarrow \infty$  (3). All other parameters are as in Fig. 1.

The slope of this line indicates that the number of ligands in the complex is 0.58. The physical meaning of this number is that 58% of the complex is dissociated during the voltammetric measurement. If  $\rho = 0.5$  the slope of the straight line (2) is -0.023 V, which indicates that the number of ligands is 0.39. This means that the complex appears less dissociated if the parameter  $\rho$  is bigger. However, the stability constants that are determined from the cross sections of straight lines (1) and (2) do not depend on  $\rho$  significantly:  $\log K_{sq} = 2.94$  if  $\rho = 0.03$  and  $\log K_{sq} = 3$  if  $\rho = 0.5$ .

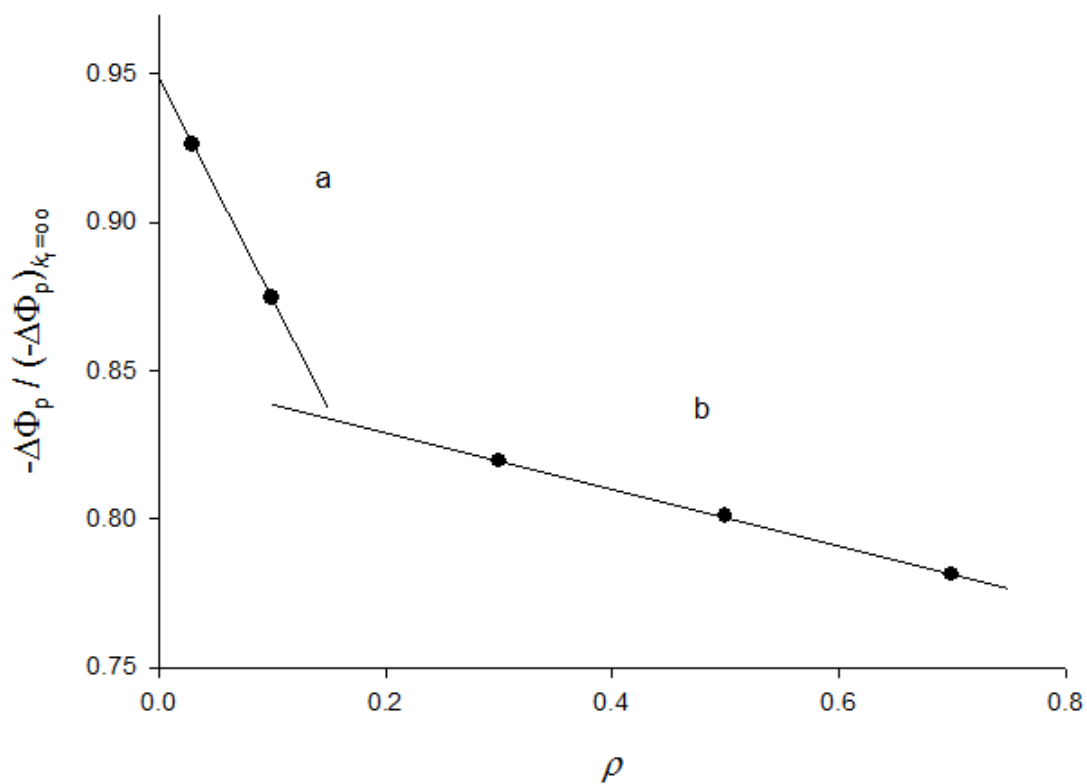
Figure 5 shows the dependence of net peak currents on the dimensionless rate constant of dissociation of complex. Within the interval  $0.01 < k_f/f < 6$  these relationships satisfy a general equation:

$$-\Delta\Phi_p = (-\Delta\Phi_p)_{k_f=0} + (-\Delta\Phi_p)_{k_f \rightarrow \infty} (k_f/f)^q (1 + (k_f/f)^q)^{-1} \quad (21)$$

The exponent  $q$  depends on the sphericity parameter:  $q = 0.5$  ( $\rho = 0.03$ ), 0.57 ( $\rho = 0.1$ ), 0.71 ( $\rho = 0.3$ ) and 0.77 ( $\rho \geq 0.5$ ). The values of  $(-\Delta\Phi_p)_{k_f \rightarrow \infty}$  are reported as the short lines at the right edge of the figure. One can notice that the difference between  $-\Delta\Phi_p$  that is calculated for the highest value of the kinetic parameter  $k_f/f$  and the corresponding  $(-\Delta\Phi_p)_{k_f \rightarrow \infty}$  is bigger if  $\rho$  is bigger. This is quantified in Fig. 6A in which the ratio  $-\Delta\Phi_p / (-\Delta\Phi_p)_{k_f \rightarrow \infty}$  is shown as a function of the sphericity parameter  $\rho$ .



**Figure 5.** Relationship between net peak currents and the dimensionless dissociation rate constant:  $\rho = 0.03$  (1), 0.1 (2), 0.3 (3), 0.5 (4) and 0.7 (5). All other parameters are as in Fig. 1.



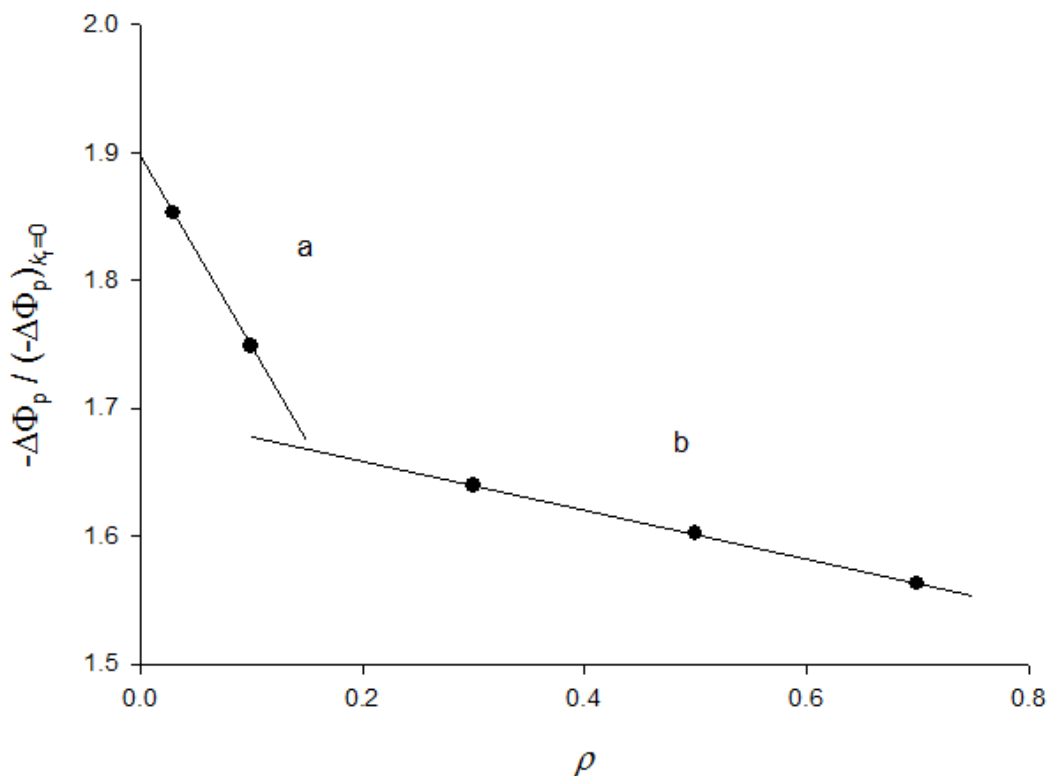


**Figure 6.** An influence of dimensionless inverse electrode radius on the ratio of net peak current and the limiting net peak current for ideally labile (A) and totally inert complex (B);  $k_f/f = 8.5$  and all other parameters as in Fig. 1.

This relationship consists of two straight lines, one for  $\rho < 0.2$  and the other for  $\rho > 0.2$ :

$$-\Delta\Phi_p / (-\Delta\Phi_p)_{k_f \rightarrow \infty} = -0.74 \rho + 0.95 \tag{22}$$

$$-\Delta\Phi_p / (-\Delta\Phi_p)_{k_f \rightarrow \infty} = -0.10 \rho + 0.85 \tag{23}$$

Fig. 6B shows that the dependence of the ratio  $-\Delta\Phi_p / (-\Delta\Phi_p)_{k_f=0}$  on the parameter  $\rho$  can be

also described by two straight lines:

$$-\Delta\Phi_p / (-\Delta\Phi_p)_{k_f=0} = -1.48 \rho + 1.90 \tag{24}$$

$$-\Delta\Phi_p / (-\Delta\Phi_p)_{k_f=0} = -0.19 \rho + 1.70 \tag{25}$$

The limiting currents  $(-\Delta\Phi_p)_{k_f \rightarrow \infty}$  and  $(-\Delta\Phi_p)_{k_f=0}$  depend solely on the diffusion, while  $-\Delta\Phi_p$  is caused by both diffusion and dissociation. Fig. 6 demonstrates that for the same dimensionless rate constant and the same concentrations of metal and ligand, the contribution of the dissociation to the mixed flux is smaller if  $\rho$  is bigger. This means that the complex appears more inert if the electrode radius is smaller.

#### 4. CONCLUSIONS

These results show that the apparent lability of metal complex depends on the radius of spherical microelectrode. The shift of peak potential with the logarithm of ligand concentration

indicates higher number of ligands in the complex if the radius of electrode is bigger. Also, the degree of dissociation of complex apparently decreases with the increasing sphericity parameter. So, the complex may appear less labile at microelectrode than at macroelectrode.

APPENDIX:

Dimensionless concentrations are defined as follows:  $c_{ml}(k, i) = (c_{ML})_{k,r_i} / c_{tot}^*$ ,

$cm(k, i) = (c_M)_{k,r_i} / c_{tot}^*$ ,  $cl(k, i) = (c_L)_{k,r_i} / c_{tot}^*$  and  $cmhg(k, i) = (c_{M(Hg)})_{k,r_i} / c_{tot}^*$ , where

$c_{tot}^* = c_M^* + c_{ML}^*$ . Dimensionless current  $w = I\Delta t(nFS c_{tot}^* \Delta r)^{-1}$  is calculated by the following formulae:

$$w_k = 2d[cmhg(k, m)exp(\varphi_k) - cm(k, m + 1)][1 + exp(\varphi_k)]^{-1} \tag{A1}$$

$$cm(k + 1, m + 1) = cm(k, m + 1)(1 - 3d \times fd(m + 1)) + 3d \times fd(m + 1)cm(k, m + 2) + 3fl(m + 1)w_k + k_f \Delta t \times c_{ml}(k, m + 1) - k_b^* cm(k, m + 1)cl(k, m + 1) \tag{A2}$$

$$c_{ml}(k + 1, m + 1) = c_{ml}(k, m + 1)(1 - 3d \times fd(m + 1)) + 3d \times fd(m + 1)c_{ml}(k, m + 2) - k_f \Delta t \times c_{ml}(k, m + 1) + k_b^* cm(k, m + 1)cl(k, m + 1) \tag{A3}$$

$$cl(k + 1, m + 1) = cl(k, m + 1)(1 - 3d \times fd(m + 1)) + 3d \times fd(m + 1)cl(k, m + 2) + k_f \Delta t \times c_{ml}(k, m + 1) - k_b^* cm(k, m + 1)cl(k, m + 1) \tag{A4}$$

$i \geq m + 2$

$$cm(k + 1, i) = cm(k, i)[1 - 3d(fd(i) + fl(i))] + 3d[fd(i)cm(k, i + 1) + fl(i)cm(k, i - 1)] + k_f \Delta t \times c_{ml}(k, i) - k_b^* cm(k, i)cl(k, i) \tag{A5}$$

$$c_{ml}(k + 1, i) = c_{ml}(k, i)[1 - 3d(fd(i) + fl(i))] + 3d[fd(i)c_{ml}(k, i + 1) + fl(i)c_{ml}(k, i - 1)] - k_f \Delta t \times c_{ml}(k, i) + k_b^* cm(k, i)cl(k, i) \tag{A6}$$

$$cl(k + 1, i) = cl(k, i)[1 - 3d(fd(i) + fl(i))] + 3d[fd(i)cl(k, i + 1) + fl(i)cl(k, i - 1)] + k_f \Delta t \times c_{ml}(k, i) - k_b^* cm(k, i)cl(k, i) \tag{A7}$$

$$cmhg(k + 1, 1) = cmhg(k, 1)(1 - 3d) + 3d \times cmhg(k, 2) \tag{A8}$$

$2 \leq i \leq m - 1$

$$cmhg(k + 1, i) = cmhg(k, i)[1 - 3d(fd(i) + fl(i))] + 3d[fd(i)cmhg(k, i + 1) + fl(i)cmhg(k, i - 1)] \tag{A9}$$

$$cmhg(k + 1, m) = cmhg(k, m)(1 - 3d \times fl(m)) + 3d \times fl(m)cmhg(k, m - 1) - 3fd(m)w_k \tag{A10}$$

$$d = D\Delta t\Delta r^{-2} \quad (\text{A11})$$

$$fd(i) = (i - (i - 1)^3 i^{-2})^{-1} \quad (\text{A12})$$

$$fl(i) = (i^3(i - 1)^{-2} - i + 1)^{-1} \quad (\text{A13})$$

$$k_b^* = k_f \Delta t K_{eq} c_{tot}^* \quad (\text{A14})$$

## ACKNOWLEDGEMENT

The financial support by the Croatian Science Foundation in the frame of the project number IP-11-2013-7379 is gratefully acknowledged.

## References

1. H. P. van Leeuwen, R. M. Town, J. Buffle, R. F. M. J. Cleven, W. Davison, J. Puy, W. H. van Reimsdijk and L. Sigg, *Environ. Sci. Technol.* 39 (2005) 8545.
2. J. Feldmann, P. Salaun and E. Lombi, *Environ. Chem.* 6 (2009) 275.
3. J. P. Pinheiro and H. P. van Leeuwen, *J. Electroanal. Chem.* 570 (2004) 69.
4. D. Omanović, C. Garnier, Y. Louis, V. Lenoble, S. Mounier and I. Pižeta, *Anal. Chim. Acta* 664 (2010) 136.
5. Y. Louis, P. Cmkuk, D. Omanović, C. Garnier, V. Lenoble, S. Mounier and I. Pižeta, *Anal. Chim. Acta* 606 (2008) 37.
6. H. P. van Leeuwen, J. Puy, J. Galceran and J. Cecilia, *J. Electroanal. Chem.* 526 (2002) 10.
7. Y. Louis, C. Garnier, V. Lenoble, S. Mounier, N. Cukrov, D. Omanović and I. Pižeta, *Mar. Chem.* 114 (2009) 110.
8. D. Omanović, *Croat. Chem. Acta* 79 (2006) 67.
9. R. Nicolau, Y. Louis, D. Omanović, C. Garnier, S. Mounier and I. Pižeta, *Anal. Chim. Acta* 618 (2008) 35.
10. H. P. van Leeuwen and J. P. Pinheiro, *J. Electroanal. Chem.* 471 (1999) 55.
11. J. Galceran, J. Puy, J. Salvador, J. Cecilia and H. P. van Leeuwen, *J. Electroanal. Chem.* 505 (2001) 85.
12. M. Lovrić and Y. I. Turyan, *Croat. Chem. Acta* 76 (2003) 189.
13. A. Molina, I. Morales and M. Lopez-Tenes, *Electrochem. Commun.* 8 (2006) 1062.
14. N. Fatouros, D. Krulic and N. Larabi, *J. Electroanal. Chem.* 549 (2003) 81.
15. A. Molina, C. Serna, F. Martinez-Ortiz and E. Laborda, *Electrochem. Commun.* 10 (2008) 376.
16. M. Rudolph, *J. Electroanal. Chem.* 503 (2001) 15.
17. M. A. Baldo, S. Daniele and G. A. Mazzocchin, *Electrochim. Acta* 41 (1996) 811.
18. V. Mirčeski, R. Gulaboski, M. Lovrić, I. Bogeski, R. Kappl and M. Hoth, *Electroanalysis* 25 (2013) 2411.
19. J. J. O'Dea, J. Osteryoung and R. A. Osteryoung, *Anal. Chem.* 53 (1981) 695.
20. K. Aoki, K. Tokuda, H. Matsuda and J. Osteryoung, *J. Electroanal. Chem.* 207 (1986) 25.
21. S. W. Feldberg, in A. J. Bard (Ed.), *Electroanalytical Chemistry*, Vol. 3, Marcel Dekker, New York, 1969, p. 199.
22. Š. Komorsky-Lovrić, M. Lovrić and A.M. Bond, *Electroanalysis* 5 (1993) 29.
23. Š. Komorsky-Lovrić, D. Jadreško and M. Lovrić, *Electrochim. Acta* 130 (2014) 286.
24. D. D. DeFord and D. N. Hume, *J. Am. Chem. Soc.* 73 (1951) 5321.